

Supporting Information for

## Achieving Tunable Cold/Warm White Light Emission in a Single Perovskite Material with Near-Unity Photoluminescence Quantum Yield

Bo Zhou<sup>1,2,‡</sup>, Aixuan Du<sup>1,‡</sup>, Dong Ding<sup>2</sup>, Zexiang Liu<sup>1</sup>, Ye Wang<sup>3</sup>, Haizhe Zhong<sup>1</sup>, Henan Li<sup>4</sup>, Hanlin Hu<sup>5,\*</sup>, Yumeng Shi<sup>4,\*</sup>

<sup>1</sup> International Collaborative Laboratory of 2D Materials for Optoelectronics Science and Technology of Ministry of Education, Institute of Microscale Optoelectronics, Shenzhen University, Shenzhen 518060, P. R. China

<sup>2</sup> Shandong Laboratory of Yantai Advanced Materials and Green Manufacturing, Yantai 264006, P. R. China

<sup>3</sup> Key Laboratory of Material Physics, Ministry of Education, School of Physics and Microelectronics, Zhengzhou University, Zhengzhou 450052, P. R. China

<sup>4</sup> School of Electronics and Information Engineering, Shenzhen University, Shenzhen 518060, P. R. China

<sup>5</sup> Hoffmann Institute of Advanced Materials, Shenzhen Polytechnic, Shenzhen 518060, P. R. China

‡ Bo Zhou and Aixuan Du contributed equally to this work.

\*Corresponding authors. E-mail: [hanlinhu@szpt.edu.cn](mailto:hanlinhu@szpt.edu.cn) (Hanlin Hu), [yumeng.shi@szu.edu.cn](mailto:yumeng.shi@szu.edu.cn) (Yumeng Shi)

### Supplementary Figures

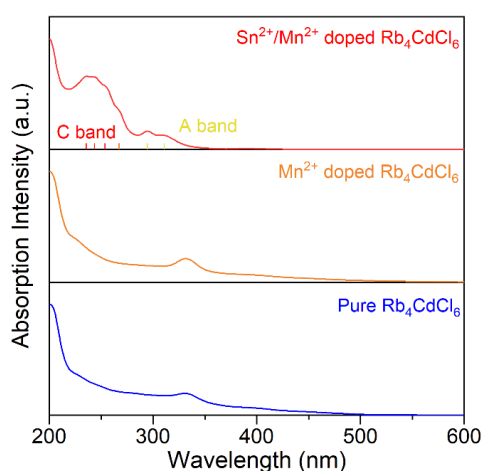


**Fig. S1** UV-vis absorption spectra of pure  $\text{Mn}^{2+}$ -doped,  $\text{Sn}^{2+}/\text{Mn}^{2+}$  co-doped  $\text{Rb}_4\text{CdCl}_6$

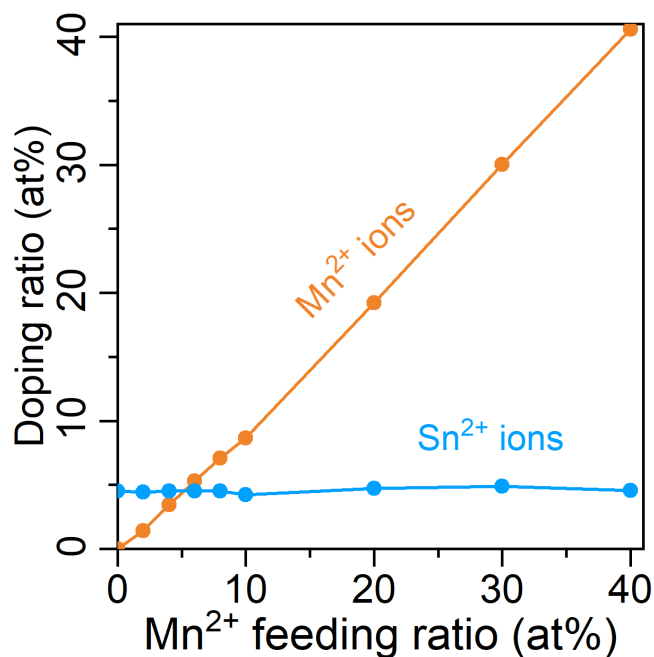


**Fig. S2** ICP-OES results for variations in  $\text{Mn}^{2+}$  doping with different feed amounts.  $\text{Sn}^{2+}$  fixed at 5%

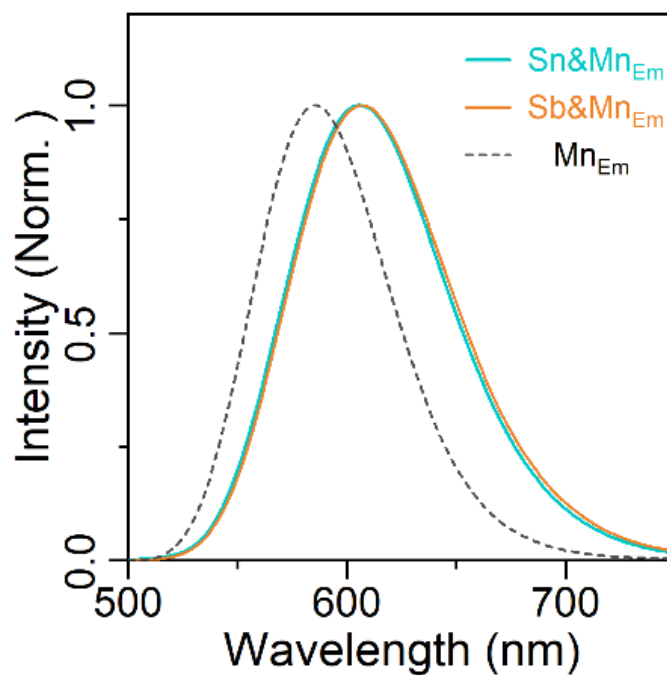


**Fig. S3** The comparison of yellow emission from  $\text{Mn}^{2+}$  doped and  $\text{Sn}^{2+}/\text{Mn}^{2+}$  co-doped  $\text{Rb}_4\text{CdCl}_6$ . It is worth noting that  $\text{Sn}^{2+}/\text{Mn}^{2+}$  and  $\text{Sb}^{3+}/\text{Mn}^{2+}$  co-doped  $\text{Rb}_4\text{CdCl}_6$  shows the similar yellow emission

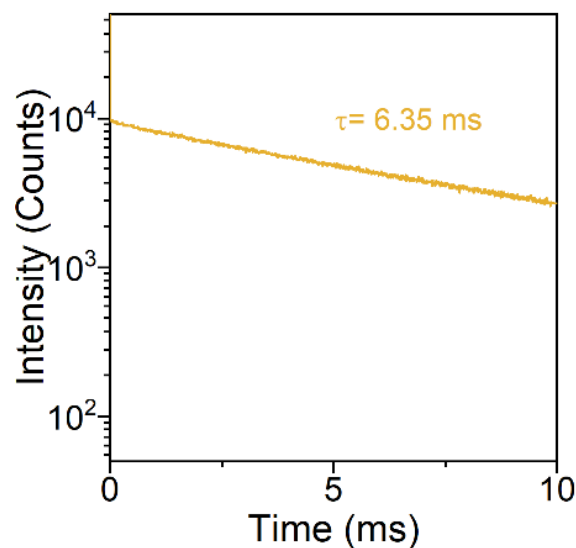


**Fig. S4** Decay curve for  $\text{Mn}^{2+}$ -doped  $\text{Rb}_4\text{CdCl}_6$  at room temperature

Interestingly, a typical 6.5 ms lifetime was observed for the  $\text{Mn}^{2+}$  doped  $\text{Rb}_4\text{CdCl}_6$  sample. However, after  $\text{Sn}^{2+}$  co-doping a significant shortening of lifetime to 4.6  $\mu\text{s}$  was observed together with the red shift of the PL peak of  $\text{Mn}^{2+}$  ions. This result indicates that  $\text{Sb}^{3+}$  has a strong effect on the emission of Mn. According to the previous reports, when Mn-based perovskites were scaled down to nanometer size, their lifetime is shortened from a few milliseconds to a few nanoseconds [S1]. The decrease of lifetime is attributed to the breaking of the forbidden transition  ${}^4\text{T}_1$  to  ${}^6\text{A}_1$ . Therefore, in this system, the forbidden  ${}^4\text{T}_1$  to  ${}^6\text{A}_1$  transition may be broken by the effect of SOC or  $ns^2$  electrons of the heavy nucleus  $\text{Sn}^{2+}$  ion. Further research is needed to reach deep understanding of the decay process.

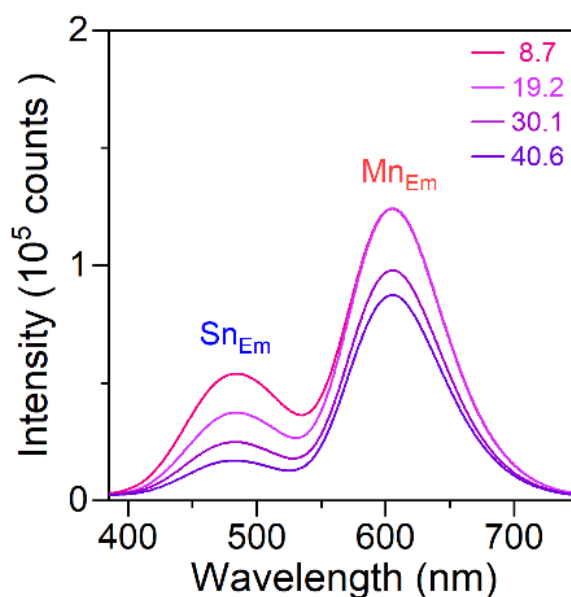


**Fig. S5** PL spectra of  $\text{Sn}^{2+}/\text{Mn}^{2+}$  co-doped samples collected by an integral sphere

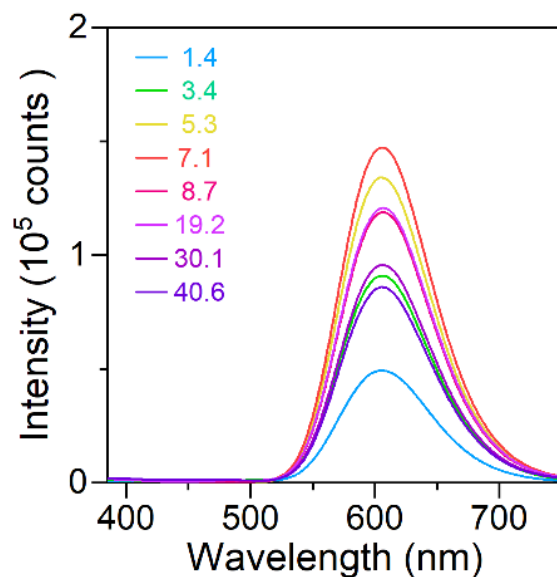


**Fig. S6**  $Mn_{Em}$  component of  $Sn^{2+}/Mn^{2+}$  co-doped samples obtained by subtracting green self-trapped exciton emission from dual emission

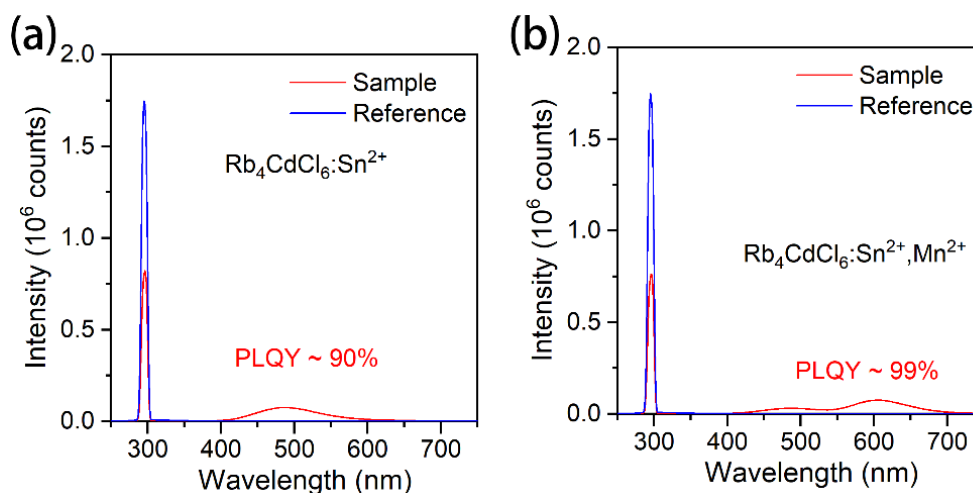


**Fig. S7** PLQY of  $Sn^{2+}$  doped and  $Sn^{2+}/Mn^{2+}$  co-doped  $Rb_4CdCl_6$  samples

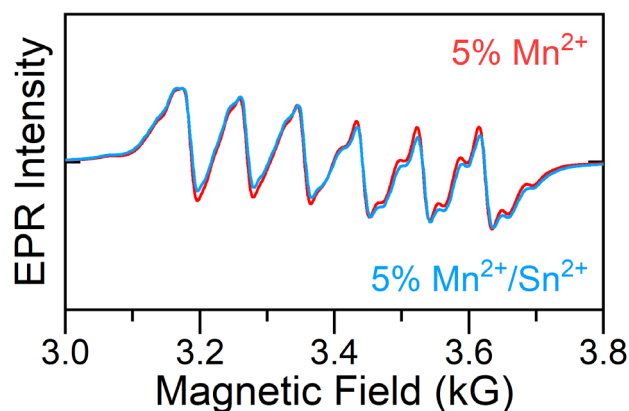


**Fig. S8** Room temperature EPR spectra of 5%  $Mn^{2+}$  doped and 5%  $Mn^{2+}/Sn^{2+}$  co-doped  $Rb_4CdCl_6$

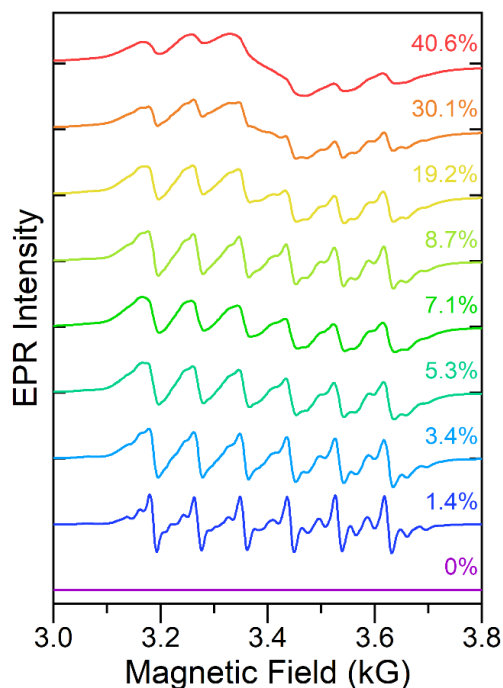


**Fig. S9** Room temperature EPR spectra of  $\text{Mn}^{2+}$  codoped  $\text{Rb}_4\text{CdCl}_6$ : 5%  $\text{Sn}^{2+}$  from 0% to 40.6%. The spectra are offset for clarity

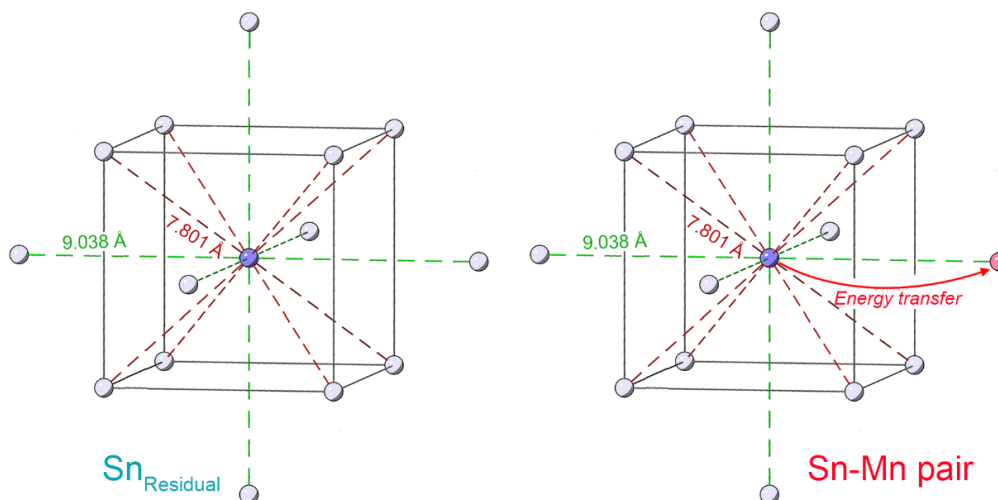


**Fig. S10** Schematic diagram of the  $\text{Sn}^{2+}$ - $\text{Mn}^{2+}$  pair in  $\text{Rb}_4\text{CdCl}_6$  structure and the calculation of residual  $\text{Sn}^{2+}$ . Each Cd sites is surrounded by 8 first nearest and 6 second nearest Cd-sites.  $\text{Rb}^+$  and  $\text{Cl}^-$  ions are hidden in the diagram

**The derivation of this probability formula:** Considering the very low doping of  $\text{Sb}^{3+}$ , assuming that there is only one site around  $\text{Sb}^{3+}$  for  $\text{Mn}^{2+}$ , the probability of Mn not occupying the site is  $(1-\text{Mn}\%)$ . In case of two sites, the value is  $(1-\text{Mn}\%)(1-\text{Mn}\%+\delta\%)$ , where  $\delta\%$  delta represents the concentration change of  $\text{Mn}^{2+}$  caused by the doping of first  $\text{Mn}^{2+}$  ions. Considering a very small  $\delta\%$ , the formula can be simplified as  $(1-\text{Mn}\%)^2$ . Similarly, in case of  $n$  sites, the value is  $(1-\text{Mn}\%)^n$ .

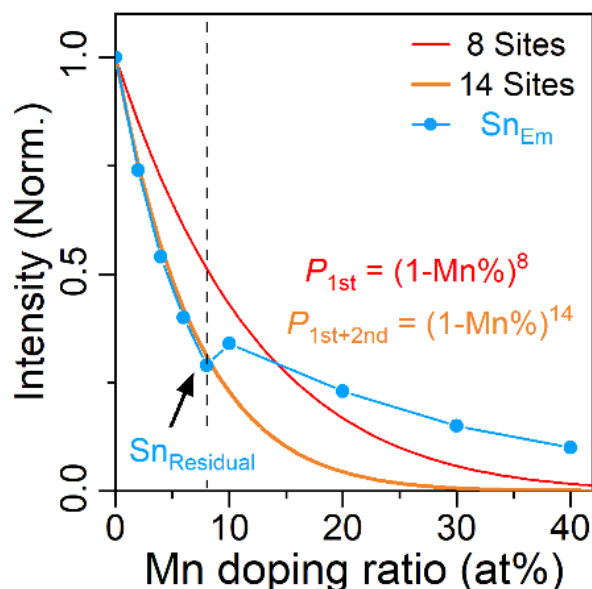


**Fig. S11** The decrease of  $\text{Sn}_{\text{Em}}$  intensity agree well with the probability of Sn nearest and second-nearest sites not being occupied by  $\text{Mn}^{2+}$

The EPR test results suggest that the Mn-Mn interaction gradually transitions from a relatively weak long-range interaction to a relatively strong short-range interaction with increasing Mn doping concentration. This suggests that as the concentration increases, adjacent  $\text{Mn}^{2+}$  and  $\text{Mn}^{2+}$  gradually become dominant. Similarly, the appearance of several  $\text{Mn}^{2+}$  adjacent to  $\text{Sn}^{2+}$  becomes significant. As a result, the competition between the Mn-Mn interaction and the Sn-Mn interaction may become significant, leading to a reduction in the energy transfer efficiency from  $\text{Sn}^{2+}$  to  $\text{Mn}^{2+}$ . This may give a slightly higher intensity for cyan emission intensity for Sn than calculated.

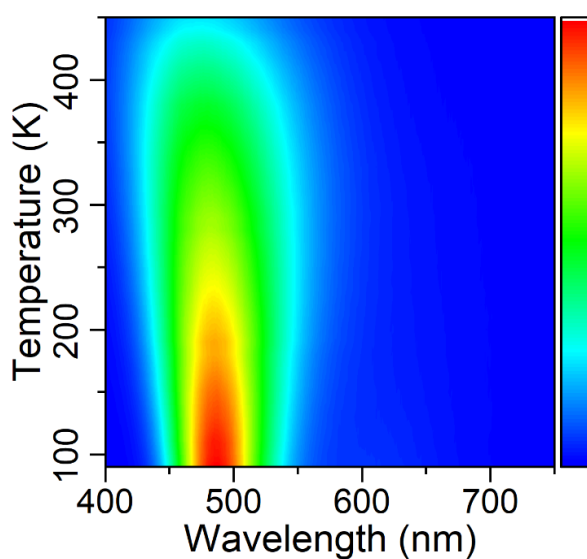


**Fig. S12** Pseudo-color maps of temperature-dependent PL from  $\text{Sn}^{2+}/\text{Mn}^{2+}$  co-doped sample in range 90–450 K

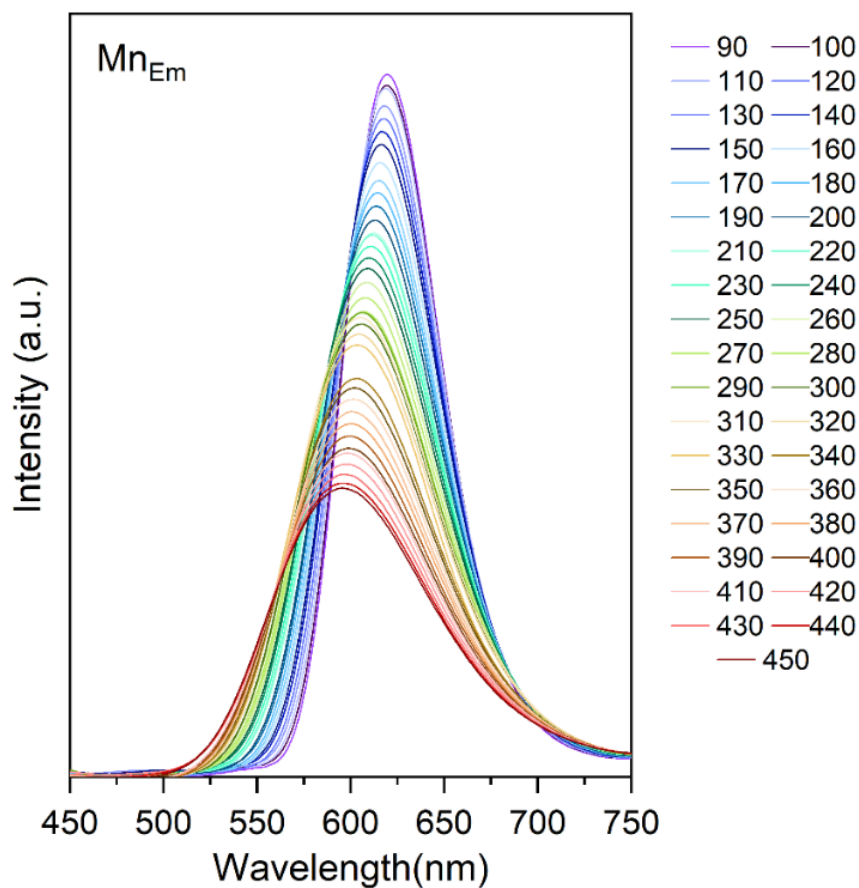


**Fig. S13** Temperature-dependent PL of the Mn<sub>Em</sub> component obtained by subtracting the cyan STE emission from the dual emission in the range 90 to 450 K

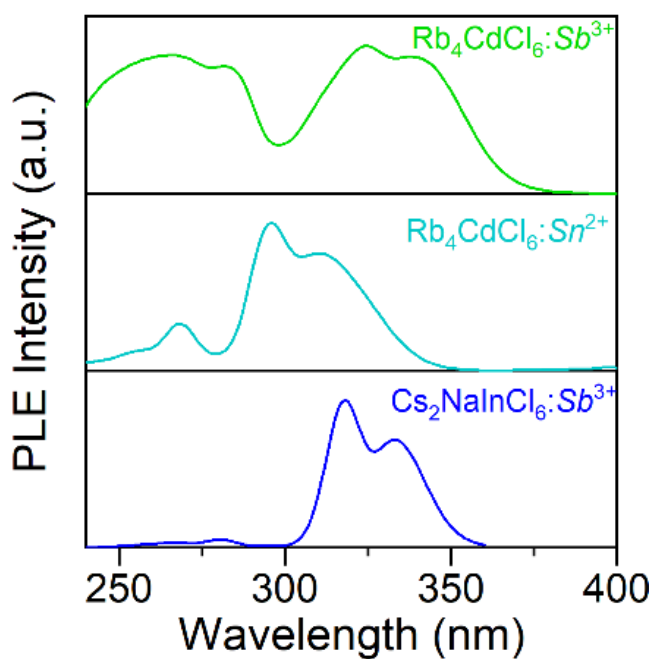


**Fig. S14** PLE spectra of  $\text{Sn}^{2+}$  doped  $\text{Rb}_4\text{CdCl}_6$  and  $\text{Sb}^{3+}$  doped  $\text{Cs}_2\text{NaInCl}_6$  and  $\text{Rb}_4\text{CdCl}_6$

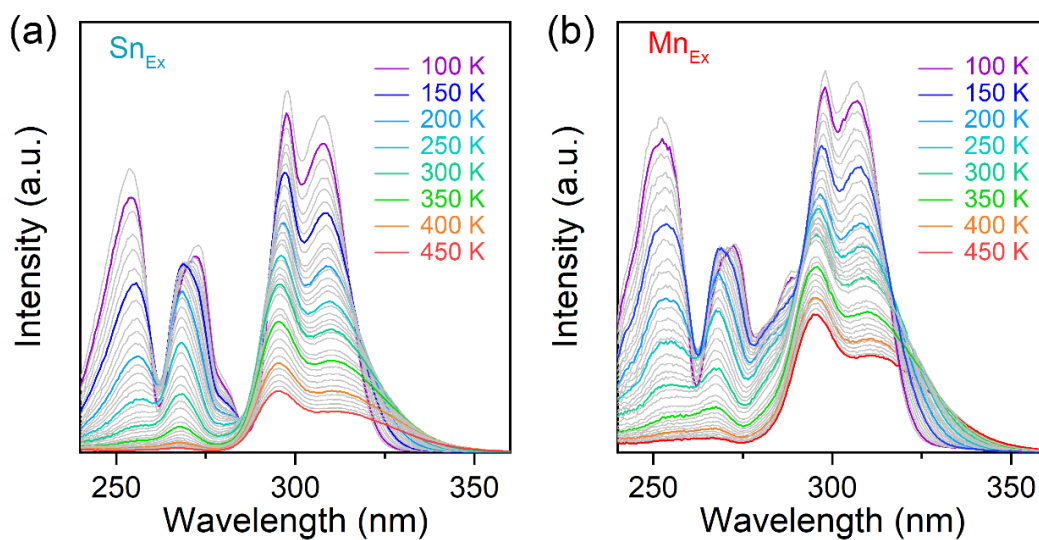


Fig. S15 Temperature dependent PLE spectra of  $\text{Sn}_{\text{Em}}$  (a) and  $\text{Mn}_{\text{Em}}$  (b) components

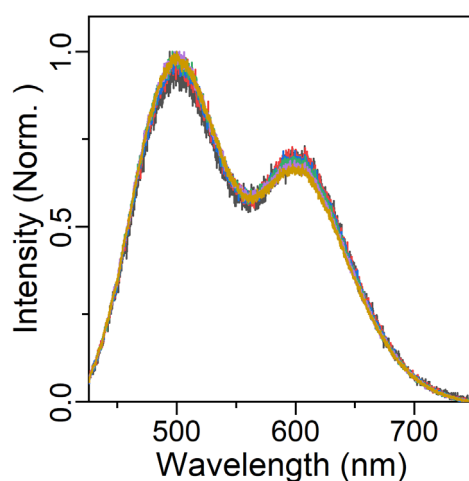


Fig. S16 Normalized emissions obtained from different currents show similar profile

Table S1 List of fitting result of A-, B- and C-bands from  $\text{Sn}_{\text{Em}}$  and  $\text{Mn}_{\text{Em}}$

	$\text{Sn}_{\text{Em}}$		$\text{Mn}_{\text{Em}}$	
	Center (nm)	FWHM (nm)	Center (nm)	FWHM (nm)
<b>A1 band</b>	310.8	33.9	309.8	36.8
<b>A2 band</b>	294.3	11.3	294.1	11.4
<b>B band</b>	-	-	283	13
<b>C1 band</b>	268.3	12.1	267.3	13
<b>C2 band</b>	254.7	12.1	253.9	13
<b>C3 band</b>	242.5	12.1	241.4	13



### **Definition of internal energy transfer efficiency:**

For short-range ET pairs, such as Sn-Mn pair, the “internal energy transfer efficiency” is defined as the ratio of the number of photons emitted by  $\text{Mn}^{2+}$  ions to the number of photons absorbed by adjacent  $\text{Sn}^{2+}$  ions. The “total energy transfer efficiency” is defined as the ratio of the number of photons emitted by  $\text{Mn}^{2+}$  ions to the number of photons absorbed by total  $\text{Sn}^{2+}$  ions. The “total energy transfer efficiency” can be obtained by averaging the “internal energy transfer efficiency” with the total  $\text{Sn}^{2+}$  ions.

### **Supplementary Reference**

[S1] J. Almutlaq, W.J. Mir, L. Gutiérrez-Arzaluz, J. Yin, S. Vasylevskyi et al., Lead-free nanocrystals with high photoluminescence quantum yield and picosecond radiative lifetime. *ACS Mater. Lett.* **3**(3), 290–297 (2021).  
<https://doi.org/10.1021/acsmaterialslett.0c00603>